Conference paper

Luís M. T. Frija*, Bruno G. M. Rocha, Maxim L. Kuznetsov, Lília I. L. Cabral, M. Lurdes S. Cristiano and Armando J. L. Pombeiro

Well-defined nickel(II) tetrazole-saccharinate complex as homogeneous catalyst on the reduction of aldehydes: scope and reaction mechanism

https://doi.org/10.1515/pac-2019-0220

Abstract: A new (tetrazole-saccharin)nickel complex is shown to be a valuable catalyst for the hydrosilative reduction of aldehydes under microwave radiation at low temperatures. With typical 1 mol% content of the catalyst (microwave power range of 5–15 W) most reactions are complete within 30 min. The Ni(II)-catalyzed reduction of aldehydes, with a useful scope, was established for the first time by using this catalyst, and is competitive with the most effective transition-metal catalysts known for such transformation. The catalyst reveals tolerance to different functional groups, is air and moisture stable, and is readily prepared in straightforward synthetic steps. Supported by experimental data and DFT calculations, a plausible reaction mechanism involving the new catalytic system is outlined.

Keywords: aldehyde reduction; DFT calculations; hydrosilylation; ICPOC-24; nickel; saccharin; tetrazole.

Introduction

Cumulative environmental concerns have led chemists to develop cleaner and sustainable reactions for chemical transformations. One of the essential questions in synthetic organic chemistry is to develop effective, selective and atom-economical reactions which can be performed under safe and mild conditions with the aid of transition metal catalysts.

Specifically, the reduction of numerous organic compounds is an essential and pervasive reaction, assuming equivalent relevance on a laboratory or industrial scale [1–3]. Sodium borohydride is one of the most used and effective reducing agents for organic compounds, massively applied since its discovery [4, 5]. Because of its popularity, thousands of tons of sodium borohydride are produced and used every year. On the other hand, hydrosilanes are equally versatile reducing agents for a diversity of organic functional groups, in particular for aldehydes and ketones [6–13]. Analogous to the borohydrides, the Si–H bond is polarized towards hydrogen permitting silanes to act as mild sources of hydride. In addition, silanes are readily accessible, as silicon is the second most abundant element in the earth's crust.

Despite the fact that direct and transfer hydrogenation [1–3, 14–26] usually requires severe reaction conditions such as high pressure and temperature and strong base as additive, hydrosilylation is classically performed under more smooth conditions [27–31]. Besides, in catalytic hydrosilylation, both the reduction of carbonyl

Article note: A collection of invited papers based on presentations at the 24th IUPAC International Conference on Physical Organic Chemistry (ICPOC 24) held in Faro, Portugal, 1–6 July 2018.

***Corresponding author: Luís M. T. Frija,** Centro de Química Estrutural (CQE), Instituto Superior Técnico, Universidade de Lisboa, Av. Rovisco Pais, 1049-001 Lisbon, Portugal, e-mail: luisfrija@tecnico.ulisboa.pt
Bruno G. M. Rocha, Maxim L. Kuznetsov and Armando J. L. Pombeiro: Centro de Química Estrutural (CQE), Instituto Superior Técnico, Universidade de Lisboa, Av. Rovisco Pais, 1049-001 Lisbon, Portugal
Lília I. L. Cabral and M. Lurdes S. Cristiano: CCMAR and Department of Chemistry and Pharmacy, F.C.T., University of Algarve, P-8005-039 Faro, Portugal

functionality and protection of the resulting alcohol in the form of silyl ethers, can be accomplished in a single step with atom economy [1, 32]. Up till now, most of the hydrosilylation reactions reported have been catalyzed by precious metals, such as gold [33–36], platinum [37, 38], silver [34, 39], iridium [40–42] and ruthenium [30, 43]. As an alternative to these metals, Cu [44–46], Fe [47, 48] and Ni [31, 49–52] have recently been applied in the reduction of the carbonyl group by hydrosilylation, typically in presence of a base or PPh_3 [34, 53–55].

In spite of the important advantages in terms of environmental and cost benefits, as compared to borohydrides, the synthetic community has not yet developed a broadly applied, simple and cheap method, for the reduction of aldehydes using silanes. The main reason for this relates to the silane reactivity which is hard to adjust [56].

Nevertheless, in this regard, alkylsilanes are usually easy to handle [57, 58] while they require forceful activation in the form of a Brønsted acid [59], Lewis acid [60, 61], Lewis base [62] or transition metal [63–66] in the reaction mixture. The catalytic processes using these additives differ, but their presence is essential to increase the hydridic nature of the hydrosilane [67]. On the other hand, silanes bearing more electronegative substituents (as halide or alkoxy) or multiple hydrides are more reactive, permitting the development of excellent protocols, yet simultaneously making them difficult to manipulate [68–71].

The first example of hydrosilylation catalyzed by a N-heterocyclic carbene (NHC) complex was reported by Herrmann in 1996 using a rhodium complex comprising a naphthyl-derived carbene ligand [72]. The synthesis of NHC-metal complexes has contributed for an increase in catalyst performance in different topics, particularly on transfer hydrogenation [73–76], oxidation [77–81], C–C cross coupling [82–87] and polymerization reactions [88–93]. Since then, much effort has been devoted to the development of robust and efficient catalysts mainly based on noble metal–NHC complexes for hydrosilylation of ketones, alkynes and alkenes [94–96].

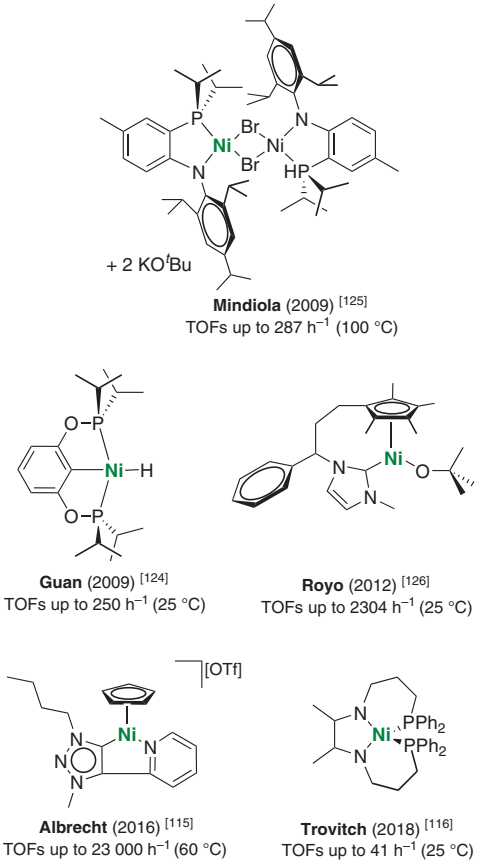

Fig. 1: Selected prominent nickel catalysts for aldehyde hydrosilylation.

In an effort to exploit Earth-abundant base metals [97–104], a series of NHC complexes of copper(I) [105–106], manganese(I) [107], and iron [108–110] were recently developed for catalyzing the hydrosilylation of carbonyl compounds. Ritleng and co-workers reported the first well-defined nickel(II) complexes bearing an imidazolylidene ligand [111], which efficiently catalyze the hydrosilylation of aldehydes and ketones at room temperature with a maximum turnover frequency of 2300 h^{-1} at 0.5 mol% catalyst loading. Successive investigations involved in particular carbene wingtip modifications afforded catalysts for the hydrosilylation of nitroarenes [112], olefins [113] and imines [114].

Besides, very recently, already in the period in which this investigation was proceeding, Albrecht and co-workers reported the synthesis of triazolylidene nickel complexes and their catalytic application in selective aldehyde hydrosilylation [115]. Even more recently, Trovitch and co-workers published an article describing the hydrosilylation of aldehydes, ketones and ester C–O bonds using κ^4-diimine nickel catalysts [116]. Homogeneous nickel compounds are recognized for the mediation of alkene hydrosilylation [117–123]; nonetheless, their trend to catalyze carbonyl hydrosilylation remains understudied. Despite everything, some nickel catalysts for aldehyde hydrosilylation have appeared in the last years showing remarkable results (see Fig. 1) [124–126].

Herein, succeeding our more recent research covering catalytic applications of tetrazole-saccharin based ligands and some of their related metal complexes [127–130], we report the discovery of a specific nickel(II) tetrazole-saccharinate complex as an excellent homogeneous catalyst for the reduction of aldehydes *via* hydrosilylation. Detailed density functional theory (DFT) calculations were also completed, supporting a probable reaction mechanism involving the new catalytic system.

Results and discussion

Tetrazolyl-type compounds can coordinate through four nitrogen electron-donating atoms and may therefore act as multidentate ligands or as a bridging building block in supramolecular assemblies. Similarly, the saccharinate anion (1,2-benzisothiazole-3-one 1,1-dioxide anion; deprotonated saccharin) interacts with metal centers in different ways, generating relatively strong interactions in crystalline environments, mostly through hydrogen bonding. As a polyfunctional ligand, it can be engaged in N, O(C=O) or O(SO_2)-metal coordination, and can also act as a bidentate amidato-like bridging agent [131–141].

In a previous work on copper- and cobalt-catalyzed alcohol oxidation reactions, the influence of a tetrazole-saccharin based ligand over the oxidation products was recognized [127]. The catalysts based on the 3-((2-methyl-2*H*-tetrazol-5-yl)amino)-benzisothiazole 1,1-dioxide (**5**) ligand were identified for efficient and selective conversion of a variety of secondary alcohols into the corresponding ketones. Short reaction times, absence of a solvent and usage of low power microwave irradiation are factors that contributed to the effectiveness of the process. In addition, molecule **5** was successfully applied as an organocatalyst on anaerobic oxidation reactions of benzyl alcohols [130].

On this basis, we started to investigate the feasibility of the synthesis of new nickel complexes based on the tetrazole-saccharin ligand **5**, with the purpose of their use as catalysts in reduction reactions. Compound **5** was prepared in three steps using a convergent synthetic strategy (Scheme 1) as previously stated by us [127]. Succeeding, the synthesis of nickel complex **6** (Scheme 1) proceeded at room temperature by reaction of ligand **5** with $Ni(OAc)_2 \cdot 4H_2O$ salt. Complex **6** was isolated as a mononuclear compound comprising two monoanionic bidentate *N*,*N*-(tetrazole-saccharin) ligands, one water and one DMSO molecule coordinated to Ni(II) ion. The complex crystallizes in the monoclinic system with space group $P2_1/c$ and the central nickel atom is hexacoordinated with a distorted octahedral N_4O_2 coordination. Detailed structural data for complex **6** can be consulted in Table 1 and Tables S1–S2 in Electronic supplementary information (ESI).

We began by investigating the influence of the solvent, reaction time, temperature and catalyst amount on the hydrosilylation of benzaldehyde (**7a**) using $PhSiH_3$ as the silane reagent (Table 2). Likewise, in sequence to other successful chemical protocols hitherto developed by us, microwave radiation was used as energy source [127, 130]. During the optimization of the reaction conditions we were pleased to find that the benzyl

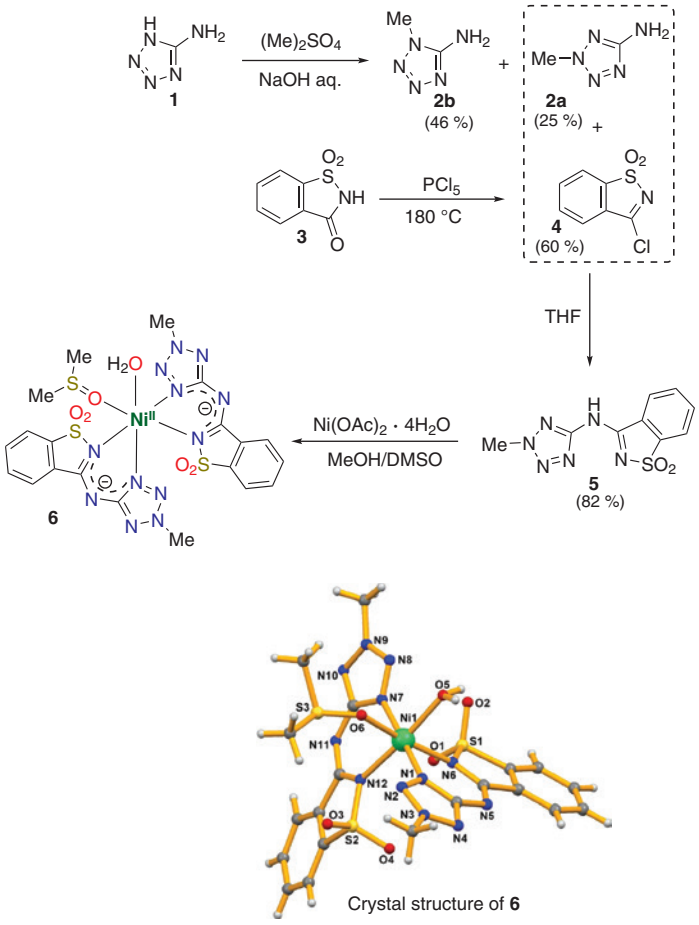

Scheme 1: Synthetic approach used for the production of nickel(II) complex **6**.

Table 1: Crystal data and structure refinement details for complex **6**.

Empirical formula	$C_{20}H_{22}N_{12}O_6S_3Ni$
Molecular weight/g mol^{-1}	681.38
Crystal system	Monoclinic
Temperature/K	297(2)
Space group	$P2_1/c$
a/Å	19.9384 (12)
b/Å	8.9196 (5)
c/Å	15.5131 (8)
α/°	90
β/°	100.244 (2)
γ/°	90
V (Å^3)	2714.9 (3)
Z	4
D_{calc} (g cm^{-3})	1.667
μ(Mo Kα)/mm^{-1}	1.01
Rfls. collected/unique/observed	44 131/5005/4013
R_{int}	0.057
Final $R1$[a], $wR2$[b] ($I \geq 2\sigma$)	0.032, 0.079
Goodness-of-fit on F^2	1.03

[a]$R = \Sigma||F_o| - |F_c||/\Sigma|F_o|$; [b]$wR(F^2) = [\Sigma w(|F_o|^2 - |F_c|^2)^2/\Sigma w|F_o|^4]^{1/2}$.

Table 2: Solvent, reaction time, temperature and catalyst amount screening for the hydrosilylation of benzaldehyde with $PhSiH_3$[a].

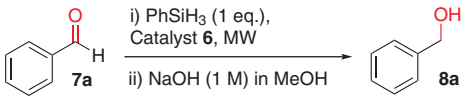

Entry	Solvent	t (min)	T (°C)	Catalyst amount (mol%)	Yield (%)[b]
1	DMF	60	80	1.0	89
2		30	80	1.0	85
3		30	80	1.5	91
4		15	80	1.0	78
5	THF	60	80	1.0	61
6		30	80	1.5	53
7	CH_3CN	60	80	1.0	55
8		30	80	1.0	30
9		60	80	1.0	96
10		60	50	1.0	91
11	DCM	30	50	1.0	92
12		30	50	1.5	95
13		15	50	1.0	78
14		60	80	1.0	90[c]
15		360	80	0.25	81
16		60	80	–	23[d]
17		60	80	1.0	78
18		60	50	1.5	80
19	DCE	30	50	1.0	81
20		30	50	2.0	77
21		15	50	1.0	55
22	*n*-Hexane	60	80	1.0	54
23		30	80	1.0	51
24	EtOH	60	80	1.0	46
25		30	80	1.0	41

[a]Reaction conditions: aldehyde **7a** (2.0 mmol), $PhSiH_3$ (2.0 mmol), solvent (1 mL) and **6**, in a microwave reactor (5–15 W) at a determined temperature. [b]Conversion into **8a** determined by use of calibrated GC methods. [c]Reaction performed with 1.5 eq. of $PhSiH_3$ (3.0 mmol). [d]Reaction performed in absence of catalyst.

alcohol (**8a**) generated by our method could be obtained in good yields for different solvents and temperatures in a short period of time.

Even, although with lower yields, the hydrosilylation of aldehyde **7a** catalyzed by complex **6** can be implemented in EtOH, a protic polar solvent (Table 2, entries 24 and 25). Increasing the stoichiometry of the silane did not provide any further beneficial effect in terms of reaction time or conversion (Table 2, entry 14).

Interestingly, **7a** undergoes reduction to **8a** with as little as 0.25 mol% (approx.) of complex **6**, although a longer reaction time is necessary (Table 2, entry 15). Nevertheless, in view of the operational easiness for small-scale reactions, the use of 1.0 mol% of **6** was considered as an optimal catalyst amount. Besides, when the reaction was done in the absence of catalyst **6**, a 23 % yield was achieved in 1 h for the transformation of benzaldehyde in DCM (Table 2, entry 16).

Thereby, based on the best results from the screening completed for delineation of optimal reaction conditions, a specific protocol was adopted for a series of aldehydes (Table 3). Typical experimental conditions used for the reduction of aldehydes *via* hydrosilylation comprised the use of one equivalent of $PhSiH_3$ and 1 mol% of the nickel catalyst (**6**) in a dichloromethane solution. The established reaction temperatures for the

Table 3: Scope of the microwave-assisted hydrosilylation of aldehydes catalyzed by nickel complex **6**[a].

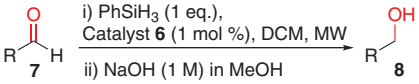

Entry	Aldehyde	t (min)	T (°C)	Yield (%)[b]	TOF (h^{-1})[c]
1	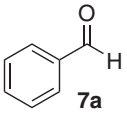 **7a**	60	50	85	89
2		60	80	94	94
3		30	50	83	184
4		15	50	70	312
5[d]		960[d]	Reflux	91	6
6	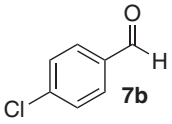 **7b**	30	50	79	158
7		60	50	85	85
8		60	80	75	75
9	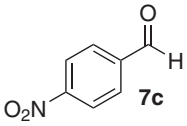 **7c**	30	50	64	128
10		60	50	67	67
11		90	80	71	47
12	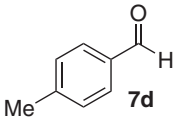 **7d**	30	50	95	190
13		15	50	85	340
14		10	80	91	546
15	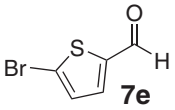 **7e**	60	50	67	67
16		30	50	61	122
17		30	80	71	142
18	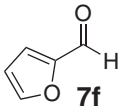 **7f**	60	50	61	61
19		30	50	52	104
20		30	80	64	128
21	**7g** 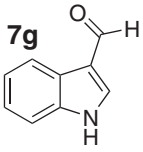	60	50	78	78
22		30	50	67	134
23		30	80	92	184
24	**7h** 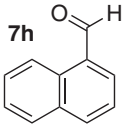	60	50	85	85
25		30	50	76	152
26		30	80	92	184
27	**7i** 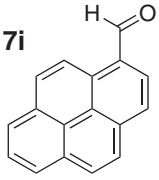	90	50	64	43
28		60	50	53	53
29		30	80	70	140
30	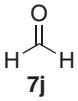 **7j**	60	50	94	94
31		30	50	87	174
32		30	80	97	194

[a]Reaction conditions: aldehyde **7** (2.0 mmol), $PhSiH_3$ (2.0 mmol), dichloromethane (1 mL) and **6** (1 mol%) in a microwave reactor (5–15 W) at a determined temperature. [b]Isolated yields. [c]TOF=TON · h^{-1}. [d]Reaction mixture heated in an oil bath.

sort of aldehydes considered varied from 50 to 80 °C corresponding to low-power microwave radiation (5–15 W). Besides, we should note that the reactions proceeded in a sealed tube into a microwave reactor and the pressure in course of the process varied in the range of 1–10 bar.

Under our chosen conditions (Table 3), **6** proved effective in enabling the high-yielding and selective reduction of various aldehydes to the corresponding primary alcohols. The *para*-substituted benzaldehyde analogues **7b–d** featured reduction in good to excellent yields for different times of reaction (Table 3, entries 6–14). For these three aldehydes, the electronic nature of the substituent group in the *para* position does not seem to be effectively striking for the reactivity shown. Nevertheless, we can infer that the presence of the electron-donating methyl group in the *para* position on aldehyde **7d** may have some effect in the formation of the silyl ether intermediary on the origin of the alcohol **8a**, since somewhat higher yields were attained in the case of such substrate (Table 3, entry 12).

Attending to the reaction yields, even though a slight decrease is noticeable, the reactivity of heterocyclic aldehydes **7e–g** (Table 3, entries 15–23) is quite similar to the benzaldehyde derivatives **7b–d**. Similarly, the reduction of aldehydes comprising extended π systems, such as naphthalene (**7h**) or pyrene (**7i**), proceeded successfully (Table 3, entries 24–29). Lastly, it was found the production of methanol by reduction of formaldehyde in almost quantitative yields (Table 3, entries 30–32).

Mechanistic studies

The knowledge of some electronic and structural properties of the nickel complex **6**, acquired by crystallographic data, allowed us to conjecture a reaction mechanism for the reduction of aldehydes *via* hydrosilylation promoted by such a metal compound. Complex **6** owns a metal oxidation state of +2, definitely the most common one for such a kind of nickel structures. The highest oxidation state of +4 is relatively infrequent in nickel intermediates [142], suggesting that the hydrosilylation possibly should not proceed by oxidative addition pathways, i.e. through formation of intermediate species based on the insertion of the aldehyde C=O bond, both at a Ni–H bond (Chalk–Harrod mechanism type) and at a Ni–Si bond (modified Chalk–Harrod mechanism type) [143, 144].

Besides, the presence of labile ligands, such as water and DMSO, in the sterically hindered complex **6**, supports a potential ligand *pseudo*-substitution on the molecule. Herein, the term *pseudo*-substitution is used to distinguish it from the classical ligand substitution. The former covalent bond among the metal centre and the ligand is really cleaved and the free coordination position is used in the formation of a non-covalent interaction between the metal centre and the silane substrate (Si–H activation), without any change in the primary nickel oxidation state.

Sustained by DFT results (discussed in more detail below) a mechanistic proposal for the reduction of aldehydes promoted by **6** was assembled and is depicted in Scheme 2 (formaldehyde appears as model substrate).

Bearing in mind that mechanisms of the type Chalk–Harrod or modified Chalk–Harrod should involve the formation of Ni(IV) species, quite unstable, these were discarded, considering to study a concerted-type outer sphere mechanism.

(i) Initial ligand elimination

The first step of the catalytic cycle should involve the elimination of a ligand, presumably water and DMSO, from the sterically hindered nickel complex (**6**). In this context, thermodynamics parameters of potential possibilities for ligand elimination were calculated (see Table S4, entries 1–9).

Although the unsaturated complexes **6′** (water elimination), **6″** (DMSO elimination) and **6‴** (water + DMSO elimination), were found to be less stable than the saturated one (**6**) (Table S3, entries 1,

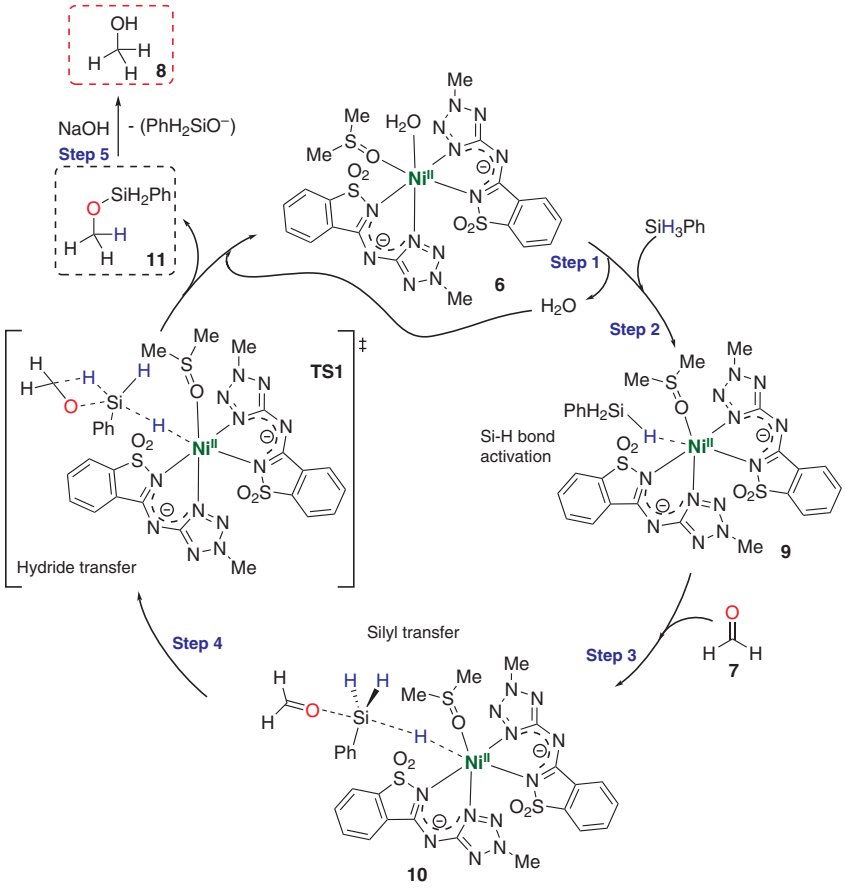

Scheme 2: Proposed mechanism for aldehyde reduction catalyzed by nickel complex **6**.

4–6), water elimination is the only spontaneous process ($\Delta G < 0$) (see Table S4, entries 1, 4 and 7). Besides, the DMSO elimination is thermodynamically non-favourable, being much less favourable than the analogous process with water (Table S4, entries 4–6 and 1–3, respectively). The conjugated elimination of water and DMSO in the same step is the less favourable among all, being the product **6'''** the less stable one as well (Table S4, entry 7).

The possibility of the first step ligand elimination from **6** to a second coordination sphere was also considered for all the discussed processes, not being favourable in any case (Table S4, entries 2, 5 and 9).

(ii) Phenylsilane activation

After the elimination of one ligand, the presence of a free coordination place in **6** leads to phenylsilane activation. Despite the results obtained in the first step of the catalytic cycle, the establishment of a non-covalent interaction between the phenylsilane and the nickel, with consequent activation of a Si–H bond, was theoretically studied for all the plausible pathways. That comprehends the water and/or DMSO elimination (Table S4, entries 10–19).

Specifically, a ligand *pseudo*-substitution from **6** to result either in the complex with the ligand in the 2nd sphere of coordination or in its elimination, as well as the reaction starting from **6** without ligand or with it at the 2nd sphere of coordination, were considered. It was verified that the processes involving the water *pseudo*-substitution are thermodynamically more favourable, comparing with those with DMSO (Table S4, entries 10–19). In fact, the stability of the intermediates in this second step follows the trend observed in the first step, where the more stables structures keep the DMSO bonded to the metal centre.

(iii) Aldehyde activation

The Si–H bond activation by nickel promotes subsequent activation of C=O bond of the formaldehyde to form the intermediate **10** (Scheme 2). From this point, and taking into account the tendency observed in the previous steps, calculations were performed only for intermediates starting from the water substitution and/or elimination in the first step. For instance, the reaction of **12** (see optimized structure at ESI) with phenylsilane is unfavourable from both a thermodynamic and a kinetic point-of-view (Table S4, entry 14). It was observed that there are no significant differences between the reaction with the water present or absent in the 2nd coordination sphere. Thus, the presence of water molecule in the 2nd coordination sphere does not facilitate the aldehyde activation, and its role is expressed at previous and later stages of the reaction.

(iv) Silyl ether formation

The interaction of C=O and Si–H bonds passes by the creation of a 4-member ring transition state (**TS1**, Scheme 2) with consequent formation of the corresponding silyl ether. At this stage, the interaction of phenylsilane with the metal centre is broken and the catalyst **6** is regenerated. The genesis of **TS1** structure was found to be the limiting step of the overall reaction with a calculated activation barrier of 23.4 kcal · mol^{-1} (Scheme 3).

(v) Silyl ether hydrolysis

This step corresponds to the formation of the desired product (alcohol) from silyl ether, that is, in fact, the product of the catalytic cycle. The silyl ether hydrolysis (using NaOH as base) does not belong to the catalytic cycle itself, once it occurs after the ether isolation. However, this step was also studied in order to enable an energetic comparison of all the reaction pathways (catalyzed or not). At this stage, the solvent used in both experimental and theoretical studies is water, where the base (OH^-) attacks the silicon nucleus to liberate PhH_2SiO^- and produce methanol. The calculated overall reaction activation barrier for the silyl ether hydrolysis is 11.9 kcal · mol^{-1} (Table S4, entry 28) and occurs *via* **TS3** transition state formation (see optimized structure at ESI).

(vi) Uncatalyzed reaction

In order to compare the catalyzed hydrosilylation with the correspondent uncatalyzed reaction, several calculations were performed in absence of catalyst. Generically, the uncatalyzed process follows a similar behaviour of the catalyzed one, with formation of a 4-member ring transition state (**TS2**, see Scheme 3) comprising the phenylsilane and the aldehyde. The genesis of **TS2** (the rate limiting step for the uncatalyzed reaction) has an activation barrier of 41.6 kcal · mol^{-1} (Table S4, entry 31). This value is substantially higher than that for the catalysed reaction (23.4 kcal · mol^{-1} Scheme 3, formation of **TS1**), demonstrating the pronounced effect of our Ni(II) catalyst. In fact, experimentally, the hydrosilylation of formaldehyde in the absence of the nickel catalyst proceeded in very low yield (see Table 2, entry 16).

Conclusions

The novel (tetrazole-saccharin)nickel complex (**6**) discovered in this study is shown to be an efficient catalyst for the hydrosilative reduction of aldehydes using microwave radiation under smooth experimental conditions. This catalyst is easily synthetized, air and moisture stable and shows a visible functional group tolerance. These characteristics further demonstrate the potential of the present nickel complex as catalyst, being competitive with analogous systems containing precious metals, provided the base metal is placed in a suitable ligand environment.

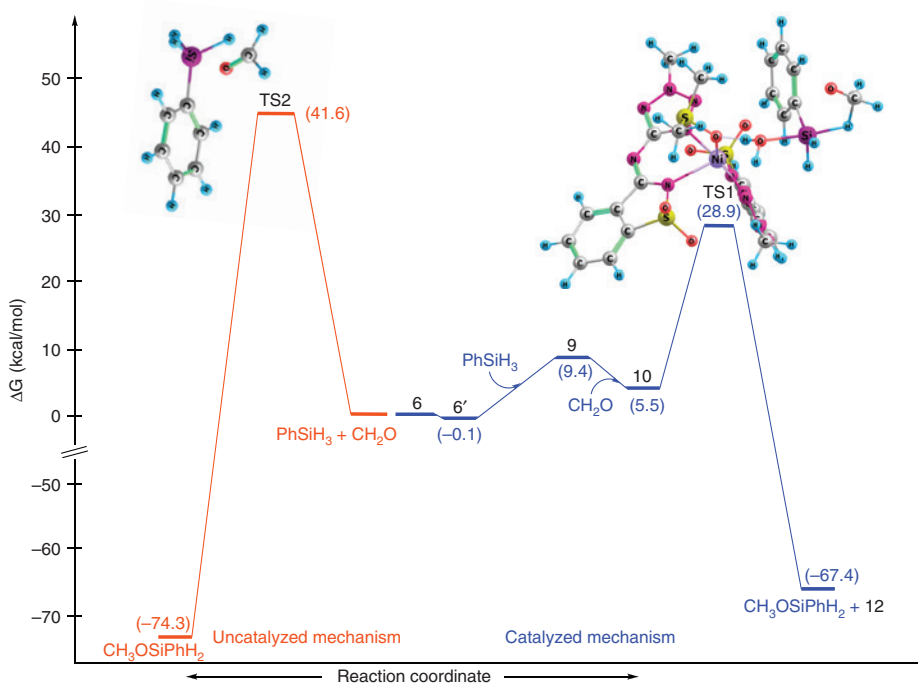

Scheme 3: Energy profile for the catalyzed (blue line) and uncatalyzed (orange line) reduction of formaldehyde *via* hydrosilylation.

Experimental section

Materials and methods

Unless indicated otherwise, solvents and starting materials were obtained from Aldrich. All chemicals used were of reagent grade without further purification before use. Column chromatography was performed using silica gel 60 MN and aluminium-backed silica gel Merck 60 F254 plates were used for analytical thin layer chromatography (TLC). Melting points were recorded and are uncorrected. ^{1}H and ^{13}C NMR spectra were recorded at room temperature on a Bruker Avance II 300 (UltraShield™ Magnet) spectrometer operating at 300 MHz (^{1}H) and 75 MHz (^{13}C). The chemical shifts are reported in ppm using TMS as internal standard. Carbon, hydrogen and nitrogen elemental analyses were carried out by the Microanalytical Service of the Instituto Superior Técnico – University of Lisbon. FT-IR spectra (4000–400 cm^{-1}) were recorded on a VERTEX 70 (Bruker) spectrometer using KBr pellets. Mass spectra were obtained on a VG 7070E mass spectrometer by electron ionization (EI) at 70 eV. Chromatographic analyses were performed in a Fisons Instruments GC 8000 series gas chromatograph with a DB-624 (J&W) capillary column (DB-WAX, column length: 30 m; internal diameter: 0.32 mm), FID detector and the Jasco-Borwin v.1.50 software; GC conditions: $T_{injection} = 240$ °C, $T_{initial} = 140$ °C (1 min) raised 10 °C min^{-1} to 220 °C (1 min), carrier gas: He.

X-ray measurements

X-ray quality single crystals of complex **6** were immersed in cryo-oil, mounted in Nylon loops and measured at a temperature of 296–297 K. Intensity data were collected using a Bruker AXS-KAPPA APEX II PHOTON 100 diffractometer with graphite monochromated Mo–Kα (λ = 0.71073) radiation. Data were collected using omega scans of 0.5° per frame and full sphere of data were obtained. Cell parameters were retrieved using

Bruker SMART [145] software and refined using Bruker SAINT [146] on all the observed reflections. Absorption corrections were applied using SADABS [124]. Structures were solved by direct methods by using SIR-97 [147] and refined with SHELXL-2014 [148]. Calculations were performed using the WinGX-Version 2014.01 [149]. The hydrogen atoms attached to carbon atoms were inserted at geometrically calculated positions and included in the refinement using the riding-model approximation; Uiso(H) were defined as 1.2 Ueq of the parent carbon atoms for phenyl residues and 1.5 Ueq of the parent carbon atoms for the methyl groups. The hydrogen atoms of water molecules were located from the final difference Fourier map and the isotropic thermal parameters were set at 1.5 times the average thermal parameters of the belonging oxygen atoms. Least square refinements with anisotropic thermal motion parameters for all the non-hydrogen atoms and isotropic for the remaining atoms were employed.

Synthesis of tetrazole-saccharin 5 and precursor compounds 2a and 4

2-Methyl-(2*H*)-tetrazole-5-amine (2a)

The molecules, 2-methyl-(2*H*)-tetrazole-5-amine (**2a**), 3-Chloro-1,2-benzisothiazole-1,1-dioxide (saccharyl chloride, **4**) and 3-((2-methyl-2*H*-tetrazol-5-yl)amino)benzisothiazole 1,1-dioxide (**5**) were synthesised following previously reported protocols [127, 150].

Synthesis of the nickel(II) complex 6

To a 10 mL methanol/dimethyl sulfoxide (DMSO) solution (1:1) of 2-methyltetrazole-saccharinate **5** (100 mg; 0.4 mmol) was added $Ni(OAc)_2 \cdot 4H_2O$ (100 mg; 0.4 mmol) and the reaction mixture was stirred for 1 h at room temperature until complete dissolution of the solids. The resulting greenish solution was kept in open air at room temperature for crystallization. After 11 days, single blue-green crystals suitable for X-ray diffraction were isolated [130 mg; 48 % yield (95 % yield based on ligand **5**)]. Elemental analysis (%): C, 35.15, H, 3.24, N, 24.58 (found); C, 35.26, H, 3.25, N, 24.67 (calculated for $C_{20}H_{22}NiN_{12}O_6S_3$). IR (KBr; cm^{-1}): 3404 ν(OH), 2919 ν(C–H), 1607, 1578, 1497, 1374 δ(CH_3), 1279 ν(C–N), 1159, 1013 ν(S=O), 958 ν(S=O), 799, 645, 558, 437.

Typical procedure for the hydrosilylation catalysis under MW irradiation

Experiments were conducted with 2.0 mmol of substrate, 2.2 mmol of $PhSiH_3$, 1 mol% of catalyst **6** and 1 mL of solvent, using a focused Anton Paar Monowave 300 microwave reactor in 10 mL glass vessels with 10 mm internal diameter, sealed with rubber membranes in a stirred mode with simultaneous cooling (IR temperature detector). A targeted temperature together with a maximum microwave power was set. The targeted temperature was reached within a few minutes. During the course of the reaction, the microwave power (5–15 W) as well as the pressure (1–10 bar) varied. Once the reaction was complete, the reaction vessel was cooled down to room temperature and then the cap was carefully opened to slowly release the pressure. After, 5 mL of a NaOH solution (1 M in MeOH) were added to the mixture, which remained under stirring at room temperature for 16 h (overnight). The organic layer was extracted with Et_2O (3 × 10 mL), dried over $MgSO_4$, filtered through a short Celite plug, and concentrated under reduced pressure. The isolated crude residue, without any further purification, was analyzed by ^{1}H-NMR.

For the particular case of the formaldehyde, after microwave reaction, the reaction solvent (dichloromethane) was primarily removed under reduced pressure. After, 0.5 mL of aqueous NaOH (1 M) were added to the mixture, which persisted under stirring at room temperature for 24 h. The methanol (reaction product) was separated from the water by distillation (Vigreux).

All of the isolated alcohols under this procedure are known compounds. Structural data for the isolated selected products are included in Electronic supplementary information (ESI).

Typical procedure for the hydrosilylation catalysis via conventional heating

To an oven-dried round-bottom flask (25 mL) equipped with a stirring bar were added DCM (5 mL) and $PhSiH_3$ (0.33 mL; 0.290 g; 2.68 mmol). The solution was stirred for 5 min. to allow complete homogenization of the silane, after which benzaldehyde (0.250 mL; 0.259 g; 2.44 mmol) and catalyst **6** (16.6 mg; 2.44×10^{-2} mmol) were added. The reaction occurred under stirring at room temperature and was monitored periodically by analysing an aliquot by TLC [hexane: diethyl ether (3:2)]. Once the reaction was complete, indicated by the disappearance of the benzaldehyde, the mixture was treated with 5 mL of a NaOH solution (1 M in MeOH) continued under stirring for 16 h. The solvent was removed under vacuum and the corresponding alcohol was extracted into Et_2O (3×10 mL). This solution was dried over $MgSO_4$, filtered through Celite and concentrated under reduced pressure to afford the corresponding alcohol (0.24 g; 91 % yield) without any further purification.

Computational details

The full geometry optimization of all structures and transition states (TS) was carried out at the DFT/HF hybrid level of theory using hybrid meta-GGA density functional M06-2X [151] with the help of the Gaussian-09 [152] program package. It was shown [153, 154] that the M06-2X functional demonstrates very good performance towards the main group thermochemistry, reasonably treating the weak dispersion forces. The *quasi*-relativistic Stuttgart-Dresden [155] pseudopotential MDF10 and the appropriate contracted basis set [156–158] were employed for the Ni atom. The Pople basis set 6-31G(d) was applied for all other atoms (C, H, N, O, Si and Si) [159–163] The geometries of all reported reactants, intermediates, transition states and products were optimized without symmetry constraints, including the solvent effect correction using the SMD model [164] with dichloromethane ($\varepsilon = 4.7113$) or water ($\varepsilon = 78.3553$), followed by analytical frequency calculations to confirm that a minimum or a transition state had been reached. The nature of the species connected by a given transition state structure was checked by IRC. Restricted approximations for the structures with closed electron shells have been employed.

Exhaustive conformational searches were performed for all intermediates and the Hessian matrix was calculated analytically for the optimized structures in order to map out the lowest energy profile and prove the location of correct minima (no imaginary frequencies) or saddle points (only one imaginary frequency) and to estimate the thermodynamic parameters, the latter being calculated at 298 K at the ideal gas conditions. The nature of all transition states was investigated by the analysis of vectors associated with the imaginary frequency and by the calculations of the intrinsic reaction coordinates (IRC) to ensure transitions states connected the illustrated ground states, using the Gonzalez-Schlegel method [165].

Single point calculations with the 6-311G(d) basis set were then performed for the equilibrium geometries found. The enthalpies and Gibbs free energies in solution (H_s and G_s) were estimated using the expressions $H_s = E_s + H_g - E_g$ and $G_s = H_s - T \bullet S_s$, where E_g and H_g are the gas-phase total energy and enthalpy. The relative energies discussed in the text are Gibbs free energies in solution if not stated otherwise. Relative Gibbs free energies (ΔG) and enthalpies (ΔH) are presented in kcal · mol^{-1}. Cartesian coordinates and total energies of all reported structures are included in ESI.

Electronic supplementary information

Table S1, with the selected bond distances and angles in the complex **6**; Table S2, with the hydrogen-bond geometry for complex **6**; The infrared spectrum of complex **6**; Structural NMR data for the isolated compounds; Table S3, with the total energies (E), enthalpies (H) and Gibbs free energies (G), for the calculated structures; Table S4, with the calculated thermodynamic parameters for the studied reactions; DFT-optimized geometries in XYZ file format, using the M06-2X functional for all the studied structures.

CCDC number 1899338 for complex **6** (Cambridge Crystallographic Data Centre via www.ccdc.cam.ac.uk/data_request/cif).

Acknowledgements: This work was partially supported by the Foundation for Science and Technology (FCT), Portugal (UID/QUI/00100/2019 and UID/MULTI/04326/2019 – CCMAR). L.M.T.F. express gratitude to FCT for the post-doc fellowship (SFRH/BPD/99851/2014: FCT Grant) and working contract n° IST-ID/115/2018: Contract. B.G.M.R. is grateful to FCT for the PhD fellowship (SFRH/BD/52370/2013: Grant; CATSUS PhD program PD/00248/2012) (UID/QUI/00100/2013: Project).

Conflicts of interest: The authors declare no conflict of interest.

References

[1] J. G. de Vries, C. J. Elsevier (Eds.). *The Handbook of Homogeneous Hydrogenation*. Wiley-VCH, Weinheim, Germany (2007).
[2] P. A. Chaloner, M. A. Esteruelas, F. Joó, L. A. Oro. *Homogeneous Hydrogenation*, p. 87, Kluwer Academic Publishers, Dordrecht (1994).
[3] R. H. Morris. *Chem. Soc. Rev.* **38**, 2282 (2009).
[4] H. I. Schlesinger, C. H. Brown, A. E. Finholt, R. J. Gilbreath, R. H. Hoekstra, K. E. Hyde. *J. Am. Chem. Soc.* **75**, 215 (1953).
[5] H. I. Schlesinger, C. H. Brown, B. Abraham, A. C. Bond, N. Davidson, A. E. Finholt, R. J. Gilbreath, H. Hoekstra, L. Horvitz, K. E. Hyde. *J. Am. Chem. Soc.* **75**, 186 (1953).
[6] G. L. Larson, J. L. Fry. *Org. React.* **71**, 1 (2008).
[7] Z. Jia, M. Liu, X. Li, A. S. C. Chan, C.-J. Li. *Synlett* **24**, 2049 (2013).
[8] M. Fujita, T. Hiyama. *J. Org. Chem.* **53**, 5405 (1988).
[9] M. P. Doyle, D. J. DeBruyn, S. J. Donnelly, D. A. Kooista, A. A. Odubeta, C. T. West, S. M. Zonnedelt. *J. Org. Chem.* **39**, 2740 (1974).
[10] M. Fujita, T. Hiyama. *J. Am. Chem. Soc.* **106**, 4629 (1984).
[11] L. Gan, M. A. Brook. *Can. J. Chem.* **84**, 1416 (2006).
[12] I. Ojima, M. Nihonyanagi, Y. Nagai. *Bull. Chem. Soc. Jpn.* **45**, 3722 (1972).
[13] H. Mimoun, J. V. de Saint Laumer, L. Giannini, R. Scopelliti, C. Floriani. *J. Am. Chem. Soc.* **121**, 6158 (1999).
[14] P. Gallezot, D. Richard. *Catal. Rev.* **40**, 81 (1998).
[15] R. Noyori, T. Ohkuma. *Angew. Chem. Int. Ed.* **40**, 40 (2001).
[16] R. Noyori. *Angew. Chem. Int. Ed.* **41**, 2008 (2002).
[17] P. Mäki-Arvela, J. Hájek, T. Salmi, D. Y. Murzin. *Appl. Catal. A* **292**, 1 (2005).
[18] J. Pritchard, G. A. Filonenko, R. van Putten, E. J. M. Hensen, E. A. Pidko. *Chem. Soc. Rev.* **44**, 3808 (2015).
[19] Y. Y. Li, S. L. Yu, W. Y. Shen, J. X. Gao. *Acc. Chem. Res.* **48**, 2587 (2015).
[20] G. Brieger, T. J. Nestrick. *Chem. Rev.* **74**, 567 (1974).
[21] G. Zassinovich, G. Mestroni, S. Gladiali. *Chem. Rev.* **92**, 1051 (1992).
[22] J. S. M. Samec, J.-E. Bäckvall, P. G. Andersson, P. Brandt. *Chem. Soc. Rev.* **35**, 237 (2006).
[23] G. Chelucci, S. Baldino, W. Baratta. *Coord. Chem. Rev.* **300**, 29 (2015).
[24] J.-I. Ito, H. Nishiyama. *Tetrahedron Lett.* **55**, 3133 (2014).
[25] D. Wang, D. Astruc. *Chem. Rev.* **115**, 6621 (2015).
[26] F. Foubelo, C. Nájera, M. Yus. *Tetrahedron: Asymmetry* **26**, 769 (2015).
[27] M. B. Smith, J. March. *March's Advanced Organic Chemistry*. Wiley-Interscience, New York (2001).
[28] B. Marciniec (Ed.). *Hydrosilylation: A Comprehensive Review on Recent Advances*. Springer, Netherlands (2009).
[29] L. Postigo, B. Royo. *Adv. Synth. Catal.* **354**, 2613 (2012).
[30] B. Chatterjee, C. Gunanathan. *Chem. Commun.* **50**, 888 (2014).
[31] S. N. MacMillan, W. H. Harman, J. C. Peters. *Chem. Sci.* **5**, 590 (2014).
[32] E. J. Corey, C. J. Helal. *Angew. Chem. Int. Ed.* **37**, 1986 (1998).
[33] H. Ito, T. Yajima, J.-I. Tateiwa, A. Hosomi. *Chem. Commun.* **11**, 981 (2000).
[34] S. Díez-González, S. P. Nolan. *Acc. Chem. Res.* **41**, 349 (2008).
[35] H. Kinoshita, R. Uemura, D. Fukuda, K. Miura. *Org. Lett.* **15**, 5538 (2013).
[36] D. Lantos, M. A. Contel, S. Sanz, A. Bodor, I. T. Horváth. *J. Organomet. Chem.* **692**, 1799 (2007).
[37] A. Kinting, H.-J. Kreuzfeld, H.-P. Abicht. *J. Organomet. Chem.* **370**, 343 (1989).
[38] J. L. Martinez, H. K. Sharma, R. Arias-Ugarte, K. H. Pannell. *Organometallics* **33**, 2964 (2014).
[39] B. M. Wile, M. Stradiotto. *Chem. Commun.* **39**, 4104 (2006).

[40] C. Cheng, M. Brookhart. *Angew. Chem. Int. Ed.* **51**, 9422 (2012).
[41] S. Park, M. Brookhart. *Organometallics* **29**, 6057 (2010).
[42] Y. Nishibayashi, K. Segawa, H. Takada, K. Ohe, S. Uemura. *Chem. Commun*. **7**, 847 (1996).
[43] Y. Nishibayashi, I. Takei, S. Uemura, M. Hidai. *Organometallics* **17**, 3420 (1998).
[44] J. T. Issenhuth, S. Dagorne, S. Bellemin-Laponnaz. *Adv. Synth. Catal.* **348**, 1991 (2006).
[45] B. H. Lipshutz, B. A. Frieman. *Angew. Chem. Int. Ed.* **44**, 6345 (2005).
[46] J. Wu, J.-X. Ji, A. S. C. Chan. *Proc. Natl. Acad. Sci. USA* **102**, 3570 (2005).
[47] T. Bleith, H. Wadepohl, L. H. Gade. *J. Am. Chem. Soc.* **137**, 2456 (2015).
[48] B. A. F. Le Bailly, S. P. Thomas. *RSC Adv.* **1**, 1435 (2011).
[49] F.-G. Fontaine, R.-V. Nguyen, D. Zargarian. *Can. J. Chem.* **81**, 1299 (2003).
[50] S. Chakraborty, J. A. Krause, H. Guan. *Organometallics* **28**, 582 (2009).
[51] B. L. Tran, M. Pink, D. J. Mindiola. *Organometallics* **28**, 2234 (2009).
[52] L. Wang, H. Sun, X. Li. *Organometallics* **34**, 5175 (2015).
[53] R. M. Bullock (Ed.). *Catalysis without Precious Metals*, p. 51, Wiley-VCH, Weinheim: Germany (2010).
[54] T. Vergote, F. Nahra, A. Merschaert, O. Riant, D. Peeters, T. Leyssens. *Organometallics* **33**, 1953 (2014).
[55] K. Revunova, G. I. Nikonov. *Chem. Eur. J* **20**, 839 (2014).
[56] Y. F. Wei, S. X. Liu, H. Mueller-Bunz, M. Albrecht. *ACS Catal.* **6**, 8192 (2016).
[57] S. Bhattacharyya. *J. Org. Chem.* **63**, 7101 (1998).
[58] T. Mizuta, S. Sakaguchi, Y. Ishii. *J. Org. Chem.* **70**, 2195 (2005).
[59] M. P. Doyle, C. T. West. *J. Org. Chem.* **40**, 3835 (1975).
[60] N. Gandhamsetty, J. Jeong, J. Park, S. Park, S. Chang. *J. Org. Chem*. **80**, 7281 (2015).
[61] S. Rendler, M. Oestreich. *Angew. Chem. Int. Ed.* **47**, 5997 (2008).
[62] A. Fedorov, A. Toutov, N. Swisher, R. Grubbs. *Chem. Sci.* **4**, 1640 (2013).
[63] M. Rubio, J. Campos, E. Carmona. *Org. Lett.* **4**, 5236 (2011).
[64] S. E. Denmark, J. D. Baird. *Chem. Eur. J.* **12**, 4954 (2006).
[65] T. T. Metsanen, M. Oestreich. *Organometallics* **34**, 543 (2015).
[66] S. Díez-González, N. M. Scott, S. P. Nolan. *Organometallics* **25**, 2355 (2006).
[67] V. Skrypai, J. J. M. Hurley, M. J. Adler. *Eur. J. Org. Chem.* **12**, 2207 (2016).
[68] H. Zhou, H. Sun, S. Zhang, X. Li. *Organometallics* **34**, 1479 (2015).
[69] K. Junge, B. Wendt, D. Addis, S. Zhou, S. Das, M. Beller. *Chem. Eur. J.* **16**, 68 (2010).
[70] S. A. Wells. *Org. Process Res. Dev.* **14**, 484 (2010).
[71] M. Zhao, W. Xie, C. Cui. *Chem. Eur. J.* **20**, 9259 (2014).
[72] W. A. Herrmann, L. J. Goossen, C. Köcher, G. R. J. Artus. *Angew. Chem. Int. Ed.* **35**, 2805 (1996).
[73] M. Poyatos, A. Maisse-François, S. Bellemin-Laponnaz, E. Peris, L. H. Gade. *J. Organomet. Chem.* **691**, 2713 (2006).
[74] W. A. Herrmann, G. D. Frey, E. Herdtweck, M. Steinbeck. *Adv. Synth. Catal.* **349**, 1677 (2007).
[75] M. Yigit, B. Yigit, I. Özdemir, E. Çetinkaya, B. Çetinkaya. *Appl. Organomet. Chem.* **20**, 322 (2006).
[76] X. Y. Yu, H. Sun, B. O. Patrick, B. R. James. *Eur. J. Inorg. Chem.* **13**, 1752 (2009).
[77] D. R. Jensen, M. J. Schultz, J. A. Mueller, M. S. Sigman. *Angew. Chem. Int. Ed.* **42**, 3810 (2003).
[78] F. Hanasaka, K.-I. Fujita, R. Yamaguchi. *Organometallics* **23**, 1490 (2004).
[79] C. N. Cornell, M. S. Sigman. *J. Am. Chem. Soc.* **127**, 2796 (2005).
[80] F. Hanasaka, K.-I. Fujita, R. Yamaguchi. *Organometallics* **25**, 4643 (2006).
[81] M. M. Konnick, B. A. Gandhi, I. A. Guzei, S. S. Stahl. *Angew. Chem. Int. Ed.* **45**, 2904 (2006).
[82] G. Altenhoff, R. Goddard, C. W. Lehmann, F. Glorius. *J. Am. Chem. Soc.* **126**, 15195 (2004).
[83] O. Navarro, R. A. Kelly, S. P. Nolan. *J. Am. Chem. Soc.* **125**, 16194 (2003).
[84] R. Ntaganda, B. Dhudshia, C. L. B. Macdonald, N. A. Thadani. *Chem. Commun*. **46**, 6200 (2008).
[85] C. Tubaro, A. Biffis, E. Scattolin, M. Basato. *Tetrahedron* **64**, 4187 (2008).
[86] V. Percec, G. M. Golding, J. Smidrkal, O. Weichold. *J. Org. Chem.* **69**, 3447 (2004).
[87] J.-I. Kuroda, K. Inamoto, K. Hiroya, T. Doi. *Eur. J. Org. Chem.* **14**, 2251 (2009).
[88] H. M. Sun, Q. Shao, D. M. Hu, W. F. Li, Q. Shen, Y. Zhang. *Organometallics* **24**, 331 (2005).
[89] B. E. Ketz, X. G. Ottenwaelder, R. M. Waymouth. *Chem. Commun*. **45**, 5693 (2005).
[90] W.-F. Li, H.-M. Sun, M.-Z. Chen, Q. Shen, Y. Zhang. *J. Organomet. Chem.* **693**, 2047 (2008).
[91] X. Wang, S. Liu, G. X. Jin. *Organometallics* **23**, 6002 (2004).
[92] W. Li, H. Sun, M. Chen, Z. Wang, D. Hu, Q. Shen, Y. Zhang. *Organometallics* **24**, 5925 (2005).
[93] S. Sujith, E. K. Noh, B. Y. Lee, J. W. Han. *J. Organomet. Chem.* **693**, 2171 (2008).
[94] M. Poyatos, A. Maisse-François, S. Bellemin-Laponnaz, L. H. Gade. *Organometallics* **25**, 2634 (2006).
[95] H. Kaur, F. K. Zinn, E. D. Stevens, S. P. Nolan. *Organometallics* **23**, 1157 (2004).
[96] A. Zanardi, E. Peris, J. A. Mata. *New J. Chem.* **32**, 120 (2008).
[97] C. E. Tucker, J. G. de Vries. *Top. Catal.* **19**, 111 (2002).
[98] B. Su, Z. C. Cao, Z. J. Shi. *Acc. Chem. Res.* **48**, 886 (2015).

[99] M. A. Asraf, H. A. Younus, M. Yusubov, F. Verpoort. *Catal. Sci. Technol.* **5**, 4901 (2015).
[100] P. Chirik, R. Morris. *Acc. Chem. Res.* **48**, 2495 (2015).
[101] I. Bauer, H.-J. Knölker, in *Iron Catalysis in Organic Chemistry*, B. Plietker (Ed.). Wiley-VCH, Weinheim: Germany (2008).
[102] M. Albrecht, R. Bedford, B. Plietker. *Organometallics* **33**, 5619 (2014).
[103] V. Ritleng, M. Henrion, M. J. Chetcuti. *ACS Catal.* **6**, 890 (2016).
[104] S. Chakraborty, H. Guan. *Dalton Trans.* **39**, 7427 (2010).
[105] A. Albright, R. E. Gawley. *J. Am. Chem. Soc.* **133**, 19680 (2011).
[106] S. R. Roy, S. C. Sau, S. K. Mandal. *J. Org. Chem.* **79**, 9150 (2014).
[107] J. Zheng, S. Elangovan, D. A. Valyaev, R. Brousses, V. César, J.-B. Sortais, C. Darcel, N. Lugan, G. Lavigne. *Adv. Synth. Catal.* **356**, 1093 (2014).
[108] S. Demir, Y. Gökçe, N. Kaloğlu, J.-B. Sortais, C. Darcel, İ. Özdemir. *Appl. Organomet. Chem.* **27**, 459 (2013).
[109] D. Bézier, F. Jiang, T. Roisnel, J.-B. Sortais, C. Darcel. *Eur. J. Inorg. Chem.* **2012**, 1333 (2012).
[110] D. Kumar, A. P. Prakasham, L. P. Bheeter, J.-B. Sortais, M. Gangwar, T. Roisnel, A. C. Kalita, C. Darcel, P. Ghosh. *J. Organomet. Chem.* **762**, 81 (2014).
[111] L. P. Bheeter, M. Henrion, L. Brelot, C. Darcel, M. J. Chetcuti, J.-B. Sortais, V. Ritleng. *Adv. Synth. Catal.* **354**, 2619 (2012).
[112] G. Vijaykumar, S. K. Mandal. *Dalton Trans.* **45**, 7421 (2016).
[113] L. Benítez Junquera, M. C. Puerta, P. Valerga. *Organometallics* **31**, 2175 (2012).
[114] L. P. Bheeter, M. Henrion, M. J. Chetcuti, C. Darcel, V. Ritleng, J.-B. Sortais. *Catal. Sci. Technol.* **3**, 3111 (2013).
[115] Y. Wei, S.-X. Liu, H. Mueller-Bunz, M. Albrecht. *ACS Catal.* **6**, 8192 (2016).
[116] C. L. Rock, T. L. Groy, R. J. Trovitch. *Dalton Trans.* **47**, 8807 (2018).
[117] Y. Chen, C. Sui-Seng, S. Boucher, D. Zargarian. *Organometallics* **24**, 149 (2005).
[118] M. I. Lipschutz, T. D. Tilley. *Chem. Commun.* **48**, 7146 (2012).
[119] A. Kuznetsov, V. Gevorgyan. *Org. Lett.* **14**, 914 (2012).
[120] T. J. Steiman, C. Uyeda. *J. Am. Chem. Soc.* **137**, 6104 (2015).
[121] I. Buslov, J. Becouse, S. Mazza, M. Montandon-Clerc, X. Hu. *Angew. Chem. Int. Ed.* **54**, 14523 (2015).
[122] I. Pappas, S. Treacy, P. J. Chirik. *ACS Catal.* **6**, 4105 (2016).
[123] Y. Nakajima, K. Sato, S. Shimada. *Chem. Rec.* **16**, 2379 (2016).
[124] S. Chakraborty, J. A. Krause, H. Guan. *Organometallics* **28**, 582 (2009).
[125] B. L. Tran, M. Pink, D. J. Mindiola. *Organometallics* **28**, 2234 (2009).
[126] L. Postigo, B. Royo. *Adv. Synth. Catal.* **354**, 2613 (2012).
[127] L. M. T. Frija, E. C. B. A. Alegria, M. Sutradhar, M. L. S. Cristiano, A. Ismael, M. N. Kopylovich, A. J. L. Pombeiro. *J. Mol. Catal. A Chem.* **425**, 283 (2016).
[128] A. Ismael, J. A. Paixão, R. Fausto, M. L. S. Cristiano. *J. Mol. Struct.* **1023**, 128 (2012).
[129] L. M. T. Frija, R. Fausto, R. M. S. Loureiro, M. L. S. Cristiano. *J. Mol. Catal. A Chem.* **305**, 142 (2009).
[130] L. M. T. Frija, M. L. Kuznetsov, B. G. M. Rocha, L. Cabral, M. L. S. Cristiano, M. N. Kopylovich, A. J. L. Pombeiro. *Mol. Catal.* **442**, 57 (2017).
[131] H. Zhao, Z.-R. Qu. *Chem. Soc. Rev.* **37**, 84 (2008).
[132] E. J. Baran, V. T. Yilmaz. *Coord. Chem. Rev.* **250**, 1980 (2006).
[133] L. M. T. Frija, A. J. L. Pombeiro, M. N. Kopylovich. *Coord. Chem. Rev.* **308**, 32 (2016).
[134] M. A. M. Abu-Youssef, F. A. Mautner, A. A. Massoud, L. Öhrström. *Polyhedron* **26**, 1531 (2007).
[135] R.-G. Xiong, X. Xue, H. Zhao, X.-Z. You, B. F. Abrahams, Z.-L. Xue. *Angew. Chem. Int. Ed.* **41**, 3800 (2002).
[136] Y.-J. Kim, Y.-S. Joo, J.-T. Han, S. H. Won, W. L. Soon. *J. Chem. Soc. Dalton Trans*. **18**, 3611 (2002).
[137] A. K. Gupta, C. H. Song, C. H. Oh. *Tetrahedron Lett.* **45**, 4113 (2004).
[138] A. S. Burukin, A. A. Vasilév, N. L. Merkulova, M. I. Struchkova, S. G. Zlotin. *Russ. Chem. Bull. Int. Ed.* **55**, 118 (2006).
[139] P. Naumov, G. Jovanovski. *Struct. Chem.* **11**, 19 (2000).
[140] F. A. Cotton, L. R. Falvello, W. Schwotzer, C. A. Murillo, G. Valle-Bourrouet. *Inorg. Chim. Acta* **190**, 89 (1991).
[141] G. Jovanovski, B. Šoptrajanov. *J. Mol. Struct.* **174**, 467 (1998).
[142] N. M. Camasso, M. S. Sanford. *Science* **347**, 1218 (2015).
[143] R. Hofmann, M. Vlatkovic, F. Wiesbrock. *Polymers* **9**, 534 (2017).
[144] N. Nakatani, J.-Y. Hasegawa, Y. Sunada, H. Nagashima. *Dalton Trans.* **44**, 19344 (2015).
[145] APES4. Bruker AXS Inc., Madison, WI (2004).
[146] SAINT. Bruker AXS Inc., Madison, WI (2004).
[147] A. Altomare, M. C. Burla, M. Camalli, G. L. Cascarano, C. Giacovazzo, A. Guagliardi, A. G. G. Moliterni, G. Polidori, R. Spagna. *J. Appl. Cryst.* **32**, 115 (1999).
[148] G. M. Sheldrick. *Acta Crystallogr. Sect. A* **64**, 112 (2008).
[149] L. J. Farrugia. *J. Appl. Crystallogr.* **32**, 837 (1999).
[150] A. F. Brigas, C. S. C. Fonseca, R. A. W. Johnstone. *J. Chem. Res.* **6**, 299 (2002).
[151] Y. Zhao, D. G. Truhlar. *Theor. Chem. Acc.* **120**, 215 (2008).
[152] M. J. Frisch, G. W. Trucks, H. B. Schlegel, G. E. Scuseria, M. A. Robb, J. R. Cheeseman, G. Scalmani, V. Barone, G. A. Petersson, H. Nakatsuji, X. Li, M. Caricato, A. Marenich, J. Bloino, B. G. Janesko, R. Gomperts, B. Mennucci, H. P. Hratchian, J.

V. Ortiz, A. F. Izmaylov, J. L. Sonnenberg, D. Williams-Young, F. Ding, F. Lipparini, F. Egidi, J. Goings, B. Peng, A. Petrone, T. Henderson, D. Ranasinghe, V. G. Zakrzewski, J. Gao, N. Rega, G. Zheng, W. Liang, M. Hada, M. Ehara, K. Toyota, R. Fukuda, J. Hasegawa, M. Ishida, T. Nakajima, Y. Honda, O. Kitao, H. Nakai, T. Vreven, K. Throssell, J. A. Montgomery, Jr., J. E. Peralta, F. Ogliaro, M. Bearpark, J. J. Heyd, E. Brothers, K. N. Kudin, V. N. Staroverov, T. Keith, R. Kobayashi, J. Normand, K. Raghavachari, A. Rendell, J. C. Burant, S. S. Iyengar, J. Tomasi, M. Cossi, J. M. Millam, M. Klene, C. Adamo, R. Cammi, J. W. Ochterski, R. L. Martin, K. Morokuma, O. Farkas, J. B. Foresman, D. J. Fox. *Gaussian 09, Revision D.01*. Gaussian, Inc., Wallingford, CT (2009).

[153] L. A. Burns, Á. Vazquez-Mayagoitia, B. G. Sumpter, C. D. Sherrill *J. Chem. Phys.* **134**, 84107 (2011).
[154] M. Sumimoto, Y. Kawashima, D. Yokogawa, K. Hori, H. Fujimoto. *J. Comput. Chem.* **32**, 3062 (2011).
[155] M. Dolg, U. Wedig, H. Stoll, H. Preuss. *J. Chem. Phys.* **86**, 866 (1987).
[156] W. Küchle, M. Dolg, H. Stoll, H. Preuss. *Mol. Phys.* **74**, 1245 (1991).
[157] D. Andrae, U. Häußermann, M. Dolg, H. Stoll, H. Preuß. *Theor. Chim. Acta* **77**, 123 (1990).
[158] A. Bergner, M. Dolg, W. Küchle, H. Stoll, H. Preuß. *Mol. Phys.* **80**, 1431 (1993).
[159] A. D. McLean, G. S. Chandler. *J. Chem. Phys.* **72**, 5639 (1980).
[160] R. Krishnan, J. S. Binkley, R. Seeger, J. A. Pople. *J. Chem. Phys.* **72**, 650 (1980).
[161] A. J. H. Wachters. *Chem. Phys.* **52**, 1033 (1970).
[162] P. J. Hay. *J. Chem. Phys.* **66**, 4377 (1977).
[163] P. C. Hariharan, J. A. Pople. *Theor. Chim. Acta* **28**, 213 (1973).
[164] G. Scalmani, M. J. Frisch. *J. Chem. Phys.* **132**, 114110 (2010).
[165] C. Gonzalez, H. B. Schlegel. *J. Chem. Phys.* **95**, 5853 (1991).

Supplementary Material: The online version of this article offers supplementary material (https://doi.org/10.1515/pac-2019-0220).